Analyst

Accepted Manuscript

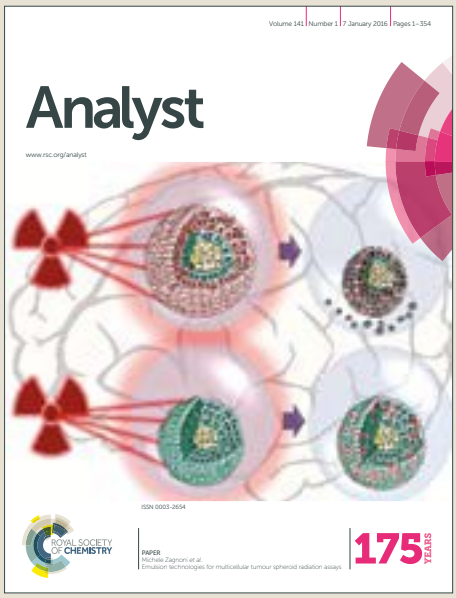

ROYAL SOCIETY OF CHEMISTRY

rsc.li/analyst

Analyst

View Article Online
DOI: 10.1039/C9AN00395A

ARTICLE

One-step rapid synthesis of fluorescent silicon nanodots for hydrogen peroxide-related sensitive and versatile assay based on inner filter effect

Received 00th January 20xx,
Accepted 00th January 20xx

DOI: 10.1039/x0xx00000x

Haoyu Chen[a], Li Wu[a], Yuqi Wan[a], Lulu Huang[a], Ningxing Li[c], Jinyang Chen[a,b]*, Guosong Lai[a]

In this work, a kind of environment-friendly and water-dispersible silicon nanodots (SiNDs) was rapidly synthesized by using the mild reagents (3-aminopropyl)triethoxysilane (APTES) and glucose. It was found that the fluorescence of as-prepared SiNDs can be quenched obviously by permanganate due to the inner filter effect. Inspired by this finding, a novel fluorescence sensor for sensitive detection of hydrogen peroxide (H_2O_2) was developed through the oxidation-reduction reaction between permanganate and H_2O_2. The detection limit of H_2O_2 is down to 2.8 nM. Since H_2O_2 is an important molecule and involved in various studies, this sensor could be applied in amounts of H_2O_2-related biological analysis. As a proof-of-application demonstration, a sensitive biosensor for glucose detection was constructed through the catalytic oxidation of glucose to generate H_2O_2. The as-constructed sensor showed good linear response to glucose over the range from 0.16 to 16 μM with a detection limit of 0.11 μM. Moreover, the biosensor can be readily extended to other sensors for different targets, which indicates the broad applications of the proposed sensing strategy in biomedical analysis.

1. Introduction

Silicon, known as the second most abundant element in the earth's crust, is the leading element and dominates the modern microelectronic and semiconductor industry. In the past years, the prosperous development of silicon nanotechnology and nanomaterial promoted silicon-related basic research and practical applications.[1-3] Among these silicon nanomaterials, silicon nanodots (SiNDs) have been drawing dramatically increasing attention in chemical and biological research in recent years.[4, 5] In addition to the advantages of rich resource support, strong fluorescence, and high photostability,[6, 7] SiNDs also feature non- or low toxicity, favorable biocompatibility and biodegradability,[8-10] which showed the potential of being powerful alternatives to the toxic heavy metal contained II-IV quantum dots and organic dyes. During the past two decades, most of the prepared SiNDs were generally terminated with hydride or halogen,[11-14] and consequently needed subsequent treatment to improve the stability and water solubility, which limited the wide-ranging applications greatly. Recently, it is realized that rapid and facile aqueous synthesis approaches for water-dispersible SiNDs would be favorable for further exploration of their applications in biochemical research. For instance, He et al. successfully developed various strategies for direct preparation of highly fluorescent SiNDs in the aqueous phase assisted with microwave or UV irradiation.[15-18] Wang et al. have facilely synthesized water-dispersible green-emitting SiNDs at room temperature by using the ascorbate sodium as reductant.[19] Nevertheless, more efforts in developing simple, fast and facile synthesis methods for water-dispersible SiNDs are still desirable. What's more, the optical applications of fluorescent SiNDs were mainly focused on biological imaging,[8, 14] and sensing of a limited variety of molecules and ions (e.g., dopamine, hydrogen sulfide, metal ions, etc.).[20-22]

[a] Hubei Key Laboratory of Pollutant Analysis & Reuse Technology, College of Chemistry and Chemical Engineering, Hubei Normal University, Huangshi 435002, PR China
[b] Key Laboratory of Analytical Chemistry for Biology and Medicine (Wuhan University), Ministry of Education, Wuhan 430072, PR China
[c] College of Chemistry and Chemical Engineering, Hunan University, Changsha 410082, PR China
E-mail: chenjy@hbnu.edu.cn

View Article Online
DOI: 10.1039/C9AN00395A

So there is still much room to explore the applications of SiNDs in biological and chemical sensing, the detection of H_2O_2 and related biomolecules based on fluorescent SiNDs is even rare.

Hydrogen peroxide (H_2O_2) is an important molecule in biology. It plays critical roles in maintaining the physiological balance of organisms in the living body. Abnormal levels of H_2O_2 will lead to severe damage for protein and DNA, thus further causing various pathological events such as autoimmune diseases, neurodegeneration, or even cancers.[23-25] So the detection of H_2O_2 is of practical importance in the chemical, biological, and clinical fields. Moreover, it is known that H_2O_2 is a byproduct of catalytic oxidation reaction initiated by oxidase, such as glucose oxidase, cholesterol oxidase, uricase, as well as the main reactant for signal-readout in enzyme-linked immunosorbent assay (ELISA) or similar immunoassay. For these reasons, the propose of new methods for H_2O_2 detection can also open the new window for the sensing of biomolecules involved in catalytic oxidation reactions, and promote the development of ELISA-based medical assay.

In order to put forward new and facile aqueous-phase synthesis methods and expand the applications of fluorescent SiNDs in biochemical sensing, we proposed a kind of environment-friendly and water-dispersible SiNDs fast synthesized by using the mild reagents (3-aminopropyl)triethoxysilane (APTES) and glucose. Inspired by the finding that the fluorescence of the prepared SiNDs can be quenched obviously by permanganate because of inner filter effect, we also developed a novel fluorescence sensor for sensitive detection of hydrogen peroxide (H_2O_2) through the oxidation-reduction reaction between permanganate and H_2O_2. Since H_2O_2 is an important molecule and involved in various studies, the proposed sensor could be applied in amounts of H_2O_2-related biological analysis. In the present work, a sensitive biosensor for glucose detection was constructed as a proof-of-application demonstration, and the preliminary detection of cholesterol was successfully performed to reveal the versatility of the proposed sensing strategy. We can thus reasonably expect that the biosensing in this work will provide new insights into the detection of H_2O_2-related biomolecules and the development of fluorescent immunoassay, as well as broadening the biological applications of SiNDs.

2. Experimental

2.1. Materials and apparatus

Glucose was purchased from Sigma-Aldrich (U.S.A.). (3-aminopropyl)triethoxysilane (APTES, 99%) and potassium permanganate were purchased from Rhawn Co., Ltd. (Shanghai, China). H_2O_2 was purchased from Aladdin Industrial Inc. (Shanghai, China). Glucose oxidase, cholesterol, cholesterol oxidase (ChOx), cysteine, thrombin, fructose, sodium fluorescein, and human serum were purchased from Sigma-Aldrich (U.S.A.). All chemical reagents were of analytical grade and used without further purification.

Fluorescence spectra were obtained with an F-4700 fluorescence spectrophotometer (Hitachi, Japan). UV-vis absorption spectra were recorded by a UV-3010 spectrophotometer (Hitachi, Japan) using a 1 cm path length quartz cuvette. FTIR spectrum over the range 600-4000 cm^{-1} was recorded with a Nicolet 5700 FTIR spectrometer. Transmission electron microscopy (TEM) and high-resolution TEM (HRTEM) images were obtained with a FEI Tecnai G^2 F20 S-TWIN transmission electron microscope (U.S.A.). Energy-dispersive X-ray (EDX) spectra were obtained with field emission scanning electron microscope (Zeiss Merlin Compact). Time-resolved fluorescence decay curves were recorded with a FELIX32 system (Photon Technology International).

2.2. Preparation of fluorescent SiNDs

For the preparation of SiNDs, 1 mL of APTES (99%) was firstly mixed with 4 mL of ultrapure water. Then 1 mL of 0.24 M glucose was added into the above mixture. After blending, the mixture solution was heated to 70 ºC with water bath for 20 min to complete the reaction and obtain the SiNDs. For purification, the as-prepared SiNDs solution was

View Article Online
DOI: 10.1039/C9AN00395A

added into acetonitrile (the volume ration of SiNDs solution/acetonitrile was fixed at 1:4) to induce the precipitation of SiNDs. After centrifugation at 8000 rpm for 5 min, the collected precipitation was vacuum drying for several hours, then the purified SiNDs were obtained and stored at 4 ºC for use.

2.3. Quantum yield calculations

The quantum yield (QY) of the as-prepared SiNDs was obtained using sodium fluorescein (QY = 95% in 0.1 M NaOH aqueous solution) as the standard. According to the integrated areas of fluorescence emission and absorbance of the SiNDs and sodium fluorescein, the QY of the SiNDs could be calculated from Equation (1) below:[26]

$$\Phi_{sample} = \frac{A_{std}}{A_{sample}} \times \frac{I_{sample}}{I_{std}} \times \frac{\eta^2_{sample}}{\eta^2_{std}} \times \Phi_{std} \quad (1)$$

Φ_{std} is the QY of the standard compound. A_{std} and A_{sample} are the absorbance of the standard compound and sample at the excitation wavelength (396 nm), respectively. I_{std} and I_{sample} are the integrated areas of fluorescence emission of the standard compound and sample in the emission region of 400-600 nm, respectively. η is the refractive index of the solvent (equal to 1.33 for water).

2.4. H_2O_2 detection and glucose detection

In the analytical application, the SiNDs could be used without further purification to shorten the whole experimental time. Typically, for H_2O_2 detection, 400 μL of 20 mM glucose was mixed with 100 μL of APTES (diluted with ultrapure water in 1:3 v/v ratio) and 1 mL ultrapure water, after blending for 2 min, the mixture was incubated at 70 ºC for 20 min to complete the preparation of SiNDs. Then 300 μL of as-prepared SiNDs solution was mixed with 300 μL of 0.013 M potassium permanganate to form probe solution. After that, 400 μL of different concentrations of H_2O_2 was added into the probe solution and incubated at room temperature for 30 min, respectively. Finally, the fluorescence emission of the solution was measured by the fluorescence spectrophotometer.

For glucose detection, the SiNDs were prepared with the same procedures as mentioned above. Similarly, 300 μL of as-prepared SiNDs solution was mixed with 300 μL of 0.013 M potassium permanganate to form probe solution. The solutions of glucose and glucose oxidase were prepared with HEPES buffer (40 mM, pH = 7.0), respectively. An amount of 100 μL of glucose oxidase (2 mg·mL^{-1}) was mixed with 400 μL of different concentrations of glucose and incubated at 37 ºC for 30 min. After the catalytic oxidation reaction, 400 μL of the mixture solution was added into 600 μL of the probe solution consisted of SiNDs and potassium permanganate and incubated at room temperature for 30 min. Finally, the fluorescence emission of the solution was measured by the fluorescence spectrophotometer. For the glucose detection in complex biological environment, the human serum prechecked with glycopenia was chosen as the model of a complex biological matrix. Then different concentrations of glucose (0, 2.0, 10, 20 μM) were spiked into the 20% diluted human serum and buffer, respectively. The prepared samples were tested with the proposed method, and subsequent procedures were the same as those mentioned above.

2.5. Cholesterol detection

The cholesterol solution was firstly prepared with 100 mM phosphate buffer (pH = 6.8) containing 1.0% (v/v) triton X-100 and a suitable amount of acetone. The cholesterol oxidase solution was prepared with 100 mM phosphate buffer (pH =6.8) containing 1.0% (v/v) triton X-100. Then 250 μL of cholesterol oxidase (0.1 U·μL^{-1}) was mixed with 250 μL of cholesterol and incubated at 40 ºC for 30 min. After the catalytic oxidation reaction, 400 μL of the mixture solution was added into 600 μL of the probe solution consisted of SiNDs and potassium permanganate and incubated at room temperature for 30 min. The subsequent steps were the same as those of glucose detection.

3. Results and discussion

View Article Online
DOI: 10.1039/C9AN00395A

3.1. Preparation of fluorescent SiNDs

The preparation method of SiNDs is illustrated in Scheme 1A. The silicon source APTES was firstly mixed with the reductant glucose in a certain ratio, then the mixture solution was heating in water bath for 30 min to obtain the fluorescent SiNDs. In the synthesis process, the ratio of reactants and reaction temperature are determinant factors to the yield of SiNDs, so the concentration of glucose and the temperature of water bath were evaluated, respectively. Under the same concentration of APTES (1.67%, v/v), the fluorescence intensity of prepared SiNDs increased with the increase of glucose concentration from 16-40 mM, and then decreased when the concentration of glucose was up to 56 mM (Fig. S1, Supplementary information). So the glucose concentration was fixed at 40 mM in subsequent experiments. With the same principle, the optimum reaction temperature was explored as 70 °C (Fig. S2). Since the SiNDs are soluble in water and insoluble in acetonitrile, the purified product could be obtained through the induced precipitation of SiNDs by acetonitrile. The collected solid particles of SiNDs were faint yellow under daylight and exhibited brilliant blue color under UV irradiation (Fig. S3). Moreover, the stability against photobleaching of as-prepared SiNDs was investigated. The results showed that the fluorescence intensity was still kept as 95% of the initial intensity when the SiNDs solution was radiated by UV-light for two hours (Fig. S4), indicating the excellent photostability of the SiNDs.

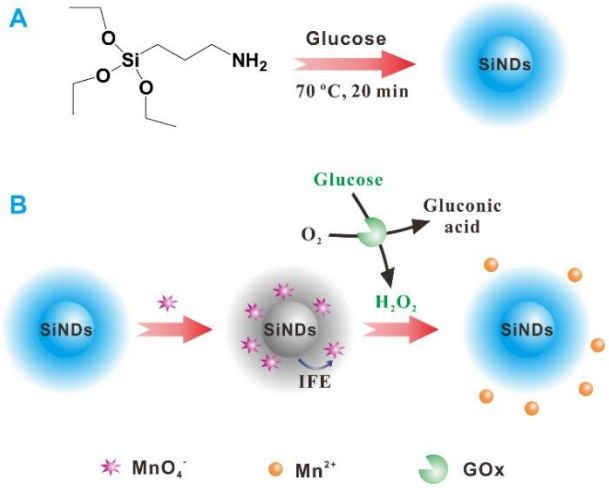

Scheme 1 Schematic illustrations of SiNDs synthesis (A) and application in the sensing of H_2O_2 and glucose (B).

3.2. Characterization of fluorescent SiNDs

To confirm the successful synthesis and investigate the characteristics of the SiNDs, the obtained product was characterized by using fluorescence spectroscopy, UV-vis absorption spectroscopy, FTIR spectroscopy, transmission electron microscopy (TEM), and EDX spectroscopy, respectively. As shown in Fig. 1A, the maximum excitation and emission wavelengths of SiNDs are 396 and 486 nm, respectively. The significant UV absorption of SiNDs appears in 350-400 nm, and has much overlap with the excitation spectrum as expect. Moreover, the resultant SiNDs sample solution is pale yellow under daylight and produces strong blue luminescence under UV irradiation (Fig. 1A, inset), indicating excellent aqueous dispersibility and high fluorescence of the resultant SiNDs. The quantum yield (QY) of the SiNDs in aqueous solution at room temperature is determined to be 22% using sodium fluorescein (QY = 95% in 0.1 M NaOH aqueous solution) as the standard, which is comparable with those of the SiNDs prepared in the previous work.[15, 19, 27] To confirm the presence of various chemical bonds in SiNDs, FTIR spectra of the as-prepared SiNDs were measured, which feature several distinct absorption peaks in the range of 1000-3500 cm^{-1} (Fig. 1B). Typically, the sharp absorbance peak at 1050 cm^{-1} is corresponding to the vibrational stretch of Si-O bonding. The strong absorbance peeks at 1595, 2928 and 3360 cm^{-1} are assigned to the N-H bending vibration, the O-H and N-H stretching vibration, respectively. It is indicated that the as-prepared SiNDs contain a large number of amino groups which is favorable to the functional modification of SiNDs. The generation of SiNDs was also evidenced by the TEM image which clearly showed that the prepared SiNDs were spherical in shape, and the average size of them was about 2.7 nm, the obvious crystal lattice structures was presented in the HRTEM image as well (Fig. 1C). The HRTEM images of SiNDs mixed with different solutions were also obtained to confirm the stability of SiNDs (Fig. S5). What's more, the elemental composition of the SiNDs was identified with EDX spectroscopy. It is indicated that the SiNDs contained Si, C, O, and N elements

(Fig. 1D).

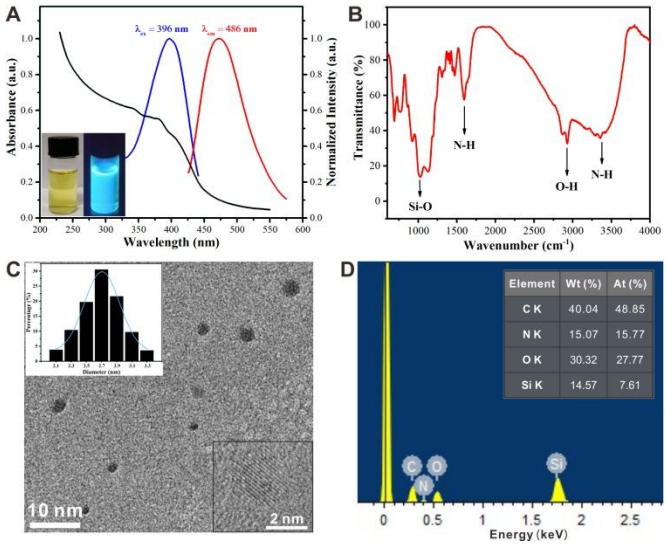

Fig. 1 (A) Fluorescence spectra and UV-vis absorption spectrum of SiNDs, insets: photographs of SiNDs aqueous solution under irradiation with daylight (left) and UV-light (right), respectively. (B) FTIR spectrum of SiNDs. (C) TEM image of SiNDs, inset: size distribution and HRTEM image of SiNDs. (D) EDX spectrum of SiNDs, inset table: elemental ratios of SiNDs.

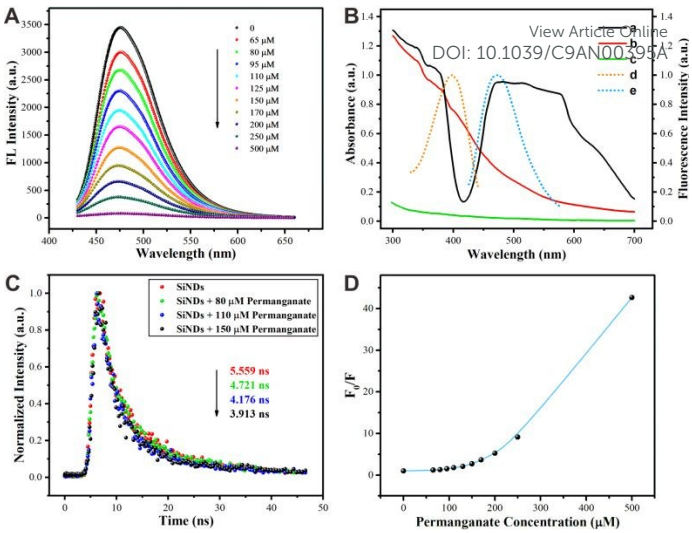

Fig. 2 (A) Fluorescence spectra of SiNDs mixed with different concentrations of permanganate. (B) UV-vis absorption spectra of MnO_4^- (a), MnO_4^- + H_2O_2 (b) and Mn^{2+} (c); fluorescence excitation spectrum (d) and emission spectrum (e) of SiNDs. (C) Time-resolved fluorescence decay curves of SiNDs mixed with different concentrations of permanganate (0, 80, 110, 150 μM). (D) Stern-Volmer plot for the fluorescence quenching of SiNDs by permanganate, F and F_0 are fluorescence intensities of the SiNDs mixed with and without permanganate, respectively.

3.3. Fluorescence quenching of SiNDs by permanganate

It was found that the fluorescence of SiNDs could be quenched by permanganate, and the fluorescence intensity of SiNDs decreased gradually with the enhancement of permanganate concentration (Fig. 2A). According to previous reports, the overlap between the absorption spectrum of the absorber and the excitation and/or emission band of the fluorophore would result in inner filter effect with high efficiency.[28, 29] In consideration of the wide UV-vis absorption range of permanganate, the fluorescence quenching of SiNDs by permanganate is most likely due to the inner filter effect. To confirm the quenching mechanism, the UV-vis absorption spectra of permanganate and fluorescence spectra of SiNDs were recorded. As shown in Fig. 2B, the absorption spectrum of permanganate hardly overlaps with the excitation spectrum of SiNDs in 380-420 nm, but overlaps with the emission spectrum of SiNDs completely in 450-520 nm. Therefore, the fluorescence quenching is mainly attributed to the inner filter effect of permanganate toward SiNDs. In addition, when the permanganate was treated with H_2O_2, the strong absorption in 450-600 nm was disappeared (Fig. 2B), which is mainly attributed to no obvious absorption for ultraviolet visible light of Mn^{2+} generated from the reaction of permanganate with H_2O_2. It means that the inner filter effect can be eliminated through the redox reaction of permanganate with H_2O_2. To further explore the quenching type, we measured the fluorescence lifetime which can be used to distinguish the dynamic quenching or static quenching.[30, 31] The time-resolved fluorescence decay curves of SiNDs in the presence of different concentrations of permanganate were shown in Fig. 2C. It is revealed that the fluorescence lifetime of SiNDs decreased with the increase of permanganate concentration, which indicating the occurrence of dynamic quenching. However, the reduction in fluorescence lifetime was not in linear proportion to the reduction in fluorescence intensity at all the three permanganate concentrations (Table S1). It means that the fluorescence quenching was not only the result

View Article Online
DOI: 10.1039/C9AN00395A

of dynamic quenching. What's more, the Stern-Volmer curve was plotted according to Stern-Volmer equation (Equation 2)

$$F_0/F = 1 + K_{SV}[Q] \qquad (2)$$

F and F_0 are fluorescence intensities of the SiNDs mixed with and without permanganate, respectively. K_{SV} is the quenching constant. $[Q]$ is the concentration of permanganate. As shown in Fig. 2D, the curve is not a straight line, but a bending line concaving toward the y-axis, which confirmed that the fluorescence quenching was result from the combination of dynamic and static quenching. The coexistence of both dynamic and static quenching might also explain the highly efficient fluorescence quenching of SiNDs by permanganate, which is just favorable to construct the quenching-and-recovery based sensor.

3.4. H_2O_2 detection

As mentioned above, the fluorescence of SiNDs can be effectively quenched by permanganate due to the inner filter effect which can be easily eliminated through the redox reaction of permanganate with H_2O_2. It is reasonable to infer that the quenched fluorescence will be recovered when H_2O_2 is added into the mixed solution of SiNDs with permanganate, and the recovery degree can be modulated by H_2O_2 concentration. Besides, the inner filter effect is well-known as a simple and effective way for fluorescence modulation, also regarded as a smart approach for the design of nanocrystal-based biochemical sensors.[32, 33] Hence, in this work, a simple and novel fluorescence sensor for H_2O_2 detection was constructed, the schematic diagram is illustrated in Scheme 1B. Since the concentration of permanganate is a key factor that influences the sensor response to H_2O_2, we investigated the concentration of potassium permanganate, and fixed the optimal concentration at 3.9 mM (Fig. S6). Then the sensitivity of the as-constructed sensor was evaluated. As shown in Fig. 3A, the fluorescence signal of the sensor dramatically increased with the increase of the concentration of H_2O_2, and the fluorescence intensity versus H_2O_2 concentration was plotted at a wide concentration range from 4.0 nM to 20 μM (Fig. 3B). There is a good linear relationship (R^2 = 0.9938) between the fluorescence intensities and H_2O_2 concentrations with a detection limit of 2.8 nM (calculated from signal-to-noise ratio of 3.0). To our knowledge, the sensitivity of this sensor is superior to those of some fluorescence nanosensing method reported previously (Table S2).[34-41]

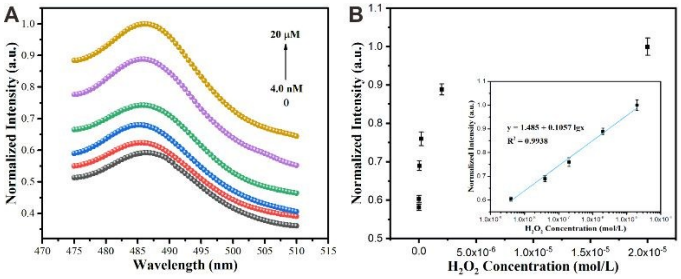

Fig. 3 (A) Fluorescence spectra of the sensor in response to the different concentrations of H_2O_2. (B) Relationship between the fluorescence intensity and H_2O_2 concentration, inset: corresponding calibration curve for H_2O_2 detection.

3.5. Glucose detection

As is known, a lot of biomolecules which play important roles in physiological reaction and human health, can be oxidized by their specific oxidases to generate H_2O_2. It means that the fluorescence sensor responded to H_2O_2 could be extended to the oxidase-based biomolecule detection. As a proof-of-application demonstration, a sensitive biosensor for glucose detection was constructed, the schematic diagram of sensing is illustrated in Scheme 1B. To evaluate the linear response range and sensitivity of glucose detection, the fluorescence emission titration experiment with increasing concentrations of glucose was carried out. As shown in Fig. 4A, the fluorescence signal gradually enhanced with the increase of glucose concentration. There is a clear linear relationship (R^2 = 0.9926) between the fluorescence intensity and the concentration of glucose over the range from 0.16 to 16 μM (Fig. 4B). It is noted that the detectable minimum concentration of 0.16 μM meets well the requirement for clinical diagnosis (threshold glucose concentration for diabetes patients is about 7 mM[42]). In addition, the limit of detection (LOD) was calculated as 0.11 μM based on the linear fitting and signal-to-noise ratio of 3.0. To the best of

View Article Online
DOI: 10.1039/C9AN00795A

our knowledge, this LOD can be comparable with or even lower than those of most fluorescence sensing strategies reported previously (Table S2).[35, 36, 39, 40, 43-45] Selectivity is also a key parameter to evaluate the sensing performance, so the experiment of recognition to different biomolecules with the as-constructed sensor was conducted. It was shown that the signal of glucose recognition was obviously stronger than those of other molecules detection (Fig. 4C). This excellent selectivity was mainly attributed to that the glucose oxidase-catalyzed oxidation reaction was triggered exclusively by the target glucose. Moreover, to evaluate the detection capability in complex biological environment, different concentrations of glucose were separately spiked into the 20% diluted human serum, and then the samples were tested with the fluorescence sensor, respectively. As shown in Fig. 4D, the fluorescence signals detected in the diluted human serum had no significant differences with those obtained in buffer, which indicated the stability of detection as well as the potentiality of real sample analysis. Such satisfactory performance of the sensor benefited from the specificity of the catalytic oxidation reaction and the reproducibility of the fluorescence quenching-recovery.

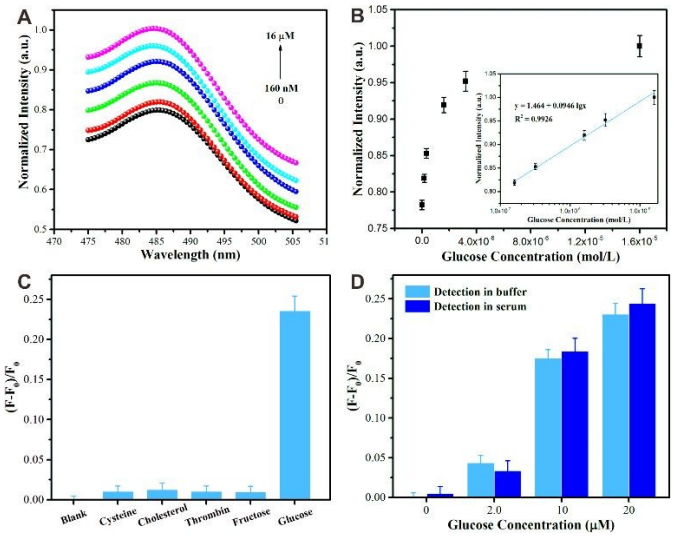

Fig. 4 (A) Fluorescence spectra of the sensing system in response to the different concentrations of glucose. (B) Relationship between the fluorescence intensity and glucose concentration, inset: corresponding calibration curve for glucose detection. (C) Fluorescence signals of the sensor responded to glucose compared to the other carbohydrates and substances. (D) Fluorescence signals of glucose detection in buffer and diluted human serum samples, respectively. F_0 is fluorescence intensity of the sensing system in the absence of target molecule, F is fluorescence intensity of the sensing system in the presence of glucose or other molecules.

3.6. Versatility of detection

To demonstrate the versatility of the fluorescence sensor in H_2O_2-related biomolecule detection, the feasibility of cholesterol detection was explored. The principle of cholesterol detection is similar to that of glucose detection just by replacing the glucose oxidase with cholesterol oxidase. As shown in Fig. 5A, when the cholesterol oxidase and cholesterol were individually added into the mixture solution of SiNDs with potassium permanganate, only weak fluorescence signal was detected, which had no obvious differences with that of adding buffer into the mixture solution. However, when cholesterol was premixed with cholesterol oxidase for sufficient reaction and then added into the mixture solution, obvious fluorescence emission was obtained, which indicated that the H_2O_2 generated from the oxidation of cholesterol by cholesterol oxidase resulted in the significant fluorescence recovery of SiNDs. What's more, with the increase of cholesterol concentration, the fluorescence signal of the sensor dramatically enhanced (Fig. 5B). Therefore, these results fully confirmed the feasibility of cholesterol detection as well as the versatility of the newly proposed sensing strategy in this work. It is reasonable to infer that other biomolecules, such as uric acid, choline and amino acid, could also be detected with the proposed sensing strategy.

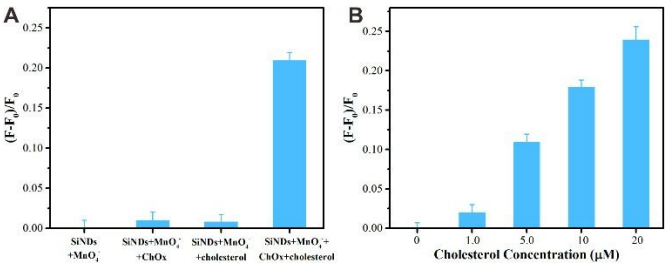

Fig. 5 (A) Fluorescence signals of the probe solution consisted of SiNDs with potassium permanganate mixed with different solutions, respectively, F_0 is fluorescence intensity of the probe solution, F is fluorescence intensity of the probe solution mixed with different solution. Cholesterol, 15 μM; Cholesterol oxidase, 0.02 U·μL^{-1}. (B) Fluorescence signals of the sensor responded to different

View Article Online
DOI: 10.1039/C9AN00395A

concentrations of cholesterol, F_0 and F are fluorescence intensities of the sensing system in the absence and presence of cholesterol. Cholesterol oxidase, 0.02 $U \cdot \mu L^{-1}$.

4. Conclusions

In summary, we put forward a new synthesis method of fluorescent SiNDs which was further applied in the construction of biochemical sensor for H_2O_2-related molecules. The successful preparation of SiNDs with mild reagents and simple operation enriched the strategies for simple, fast and facile synthesis of SiNDs. Based on the finding that the fluorescence of SiNDs can be quenched obviously by permanganate due to the inner filter effect, a novel fluorescence sensor for H_2O_2 and glucose was proposed. The as-constructed fluorescence sensor exhibits high sensitivity, selectivity and stability. In addition, this biochemical sensor could be extended to the detection of different target molecules, which indicates the versatility of the sensing strategy. Therefore, it is reasonable to expect that our efforts will provide new insights into the nanosensing of H_2O_2-related biomolecules, as well as broadening the biochemical applications of fluorescent SiNDs.

Conflicts of interest

There are no conflicts to declare.

Acknowledgements

This work was financially supported by the Science and Technology Research Project of Hubei Provincial Department of Education (Q20182504), Science and Technology Foundation for Creative Research Group of Hubei Provincial Department of Education (T201810), Key Laboratory of Analytical Chemistry for Biology and Medicine (Ministry of Education) (ACBM2018005), and Hubei Key Laboratory of Pollutant Analysis and Reuse Technique (Hubei Normal University) (PA20170208).

Notes and references

1 M. Dasog, J. Kehrle, B. Rieger and J. G. Veinot, *Angew. Chem., Int. Ed.*, 2016, 55, 2322-2339.

2 G. P. Zograf, M. I. Petrov, D. A. Zuev, P. A. Dmitriev, V. A. Milichko, S. V. Makarov and P. A. Belov, *Nano Lett.*, 2017, 17, 2945-2952.

3 S. Chandra, Y. Masuda, N. Shirahata and F. M. Winnik, *Angew. Chem., Int. Ed.*, 2017, 56, 6157-6160.

4 M. Dasog, G. B. De los Reyes, L. V. Titova, F. A. Hegmann and J. G. Veinot, *ACS Nano*, 2014, 8, 9636-9648.

5 M. Dasog, Z. Yang, S. Regli, T. M. Atkins, A. Faramus, M. P. Singh, E. Muthuswamy, S. M. Kauzlarich, R. D. Tilley and J. G. Veinot, *ACS Nano*, 2013, 7, 2676-2685.

6 Y. Zhong, B. Song, X. Shen, D. Guo and Y. He, *Chem. Commun.*, 2019, 55, 365-368.

7 Q. Li, Y. He, J. Chang, L. Wang, H. Chen, Y. W. Tan, H. Wang and Z. Shao, *J. Am. Chem. Soc.*, 2013, 135, 14924-14927.

8 M. Montalti, A. Cantelli and G. Battistelli, *Chem. Soc. Rev.*, 2015, 44, 4853-4921.

9 X. Cheng, S. B. Lowe, P. J. Reece and J. J. Gooding, *Chem. Soc. Rev.*, 2014, 43, 2680-2700.

10 S. D. Ma, Y. L. Chen, J. Feng, J. J. Liu, X. W. Zuo and X. G. Chen, *Anal. Chem.*, 2016, 88, 10474-10481.

11 T. Zhou, R. T. Anderson, H. Li, J. Bell, Y. Yang, B. P. Gorman, S. Pylypenko, M. T. Lusk and A. Sellinger, *Nano Lett.*, 2015, 15, 3657-3663.

12 P. Das, A. Saha, A. R. Maity, S. C. Ray and N. R. Jana, *Nanoscale*, 2013, 5, 5732-5737.

13 A. Shiohara, S. Prabakar, A. Faramus, C. Y. Hsu, P. S. Lai, P. T. Northcote and R. D. Tilley, *Nanoscale*, 2011, 3, 3364-3370.

14 B. F. McVey and R. D. Tilley, *Acc. Chem. Res.*, 2014, 47, 3045-3051.

15 Y. Zhong, X. Sun, S. Wang, F. Peng, F. Bao, Y. Su, Y. Li, S. T. Lee and Y. He, *ACS Nano*, 2015, 9, 5958-5967.

16 Y. Su, X. Ji and Y. He, *Adv. Mater.*, 2016, 28, 10567-10574.

17 S. Wu, Y. Zhong, Y. Zhou, B. Song, B. Chu, X. Ji, Y. Wu, Y. Su and Y. He, *J. Am. Chem. Soc.*, 2015, 137, 14726-14732.

18 Y. Zhong, F. Peng, F. Bao, S. Wang, X. Ji, L. Yang, Y. Su, S. T. Lee and Y. He, *J. Am. Chem. Soc.*, 2013, 135, 8350-8356.

19 J. Wang, D. X. Ye, G. H. Liang, J. Chang, J. L. Kong and J. Y. Chen, *J. Mater. Chem. B*, 2014, 2, 4338-4345.

20 X. Zhang, X. Chen, S. Kai, H. Y. Wang, J. Yang, F. G. Wu and Z. Chen, *Anal. Chem.*, 2015, 87, 3360-3365.

21 L. Zhu, X. Peng, H. Li, Y. Zhang and S. Yao, *Sens. Actuator B-Chem.*, 2017, 238, 196-203.

22 N. Dhenadhayalan, H. L. Lee, K. Yadav, K. C. Lin, Y. T. Lin and

View Article Online
DOI: 10.1039/C9AN00395A

A. H. Chang, *ACS Appl. Mater. Interfaces*, 2016, 8, 23953-23962.

23 C. de Gracia Lux, S. Joshi-Barr, T. Nguyen, E. Mahmoud, E. Schopf, N. Fomina and A. Almutairi, *J. Am. Chem. Soc.*, 2012, 134, 15758-15764.

24 E. A. Mazzio and K. F. Soliman, *J. Appl. Toxicol.*, 2004, 24, 99-106.

25 C. Lennicke, J. Rahn, R. Lichtenfels, L. A. Wessjohann and B. Seliger, *Cell Commun. Signal.*, 2015, 13, 39.

26 C. Wang, L. Ling, Y. Yao and Q. Song, *Nano Research*, 2015, 8, 1975-1986.

27 Y. Feng, Y. Liu, C. Su, X. Ji and Z. He, *Sens. Actuator B-Chem.*, 2014, 203, 795-801.

28 H. Liu, M. Li, Y. Xia and X. Ren, *ACS Appl. Mater. Interfaces*, 2017, 9, 120-126.

29 Y. Dong, R. Wang, G. Li, C. Chen, Y. Chi and G. Chen, *Anal. Chem.*, 2012, 84, 6220-6224.

30 Z. Gao, L. Wang, R. Su, R. Huang, W. Qi and Z. He, *Biosens. Bioelectron.*, 2015, 70, 232-238.

31 Y. Yuan, R. Li and Z. Liu, *Anal. Chem.*, 2014, 86, 3610-3615.

32 J. Zhang, X. Lu, Y. Lei, X. Hou and P. Wu, *Nanoscale*, 2017, 9, 15606-15611.

33 J. Zhang, R. Zhou, D. Tang, X. Hou and P. Wu, *TrAC Trends Anal. Chem.*, 2019, 110, 183-190.

34 T. Lin, Y. Qin, Y. Huang, R. Yang, L. Hou, F. Ye and S. Zhao, *Chem. Commun.*, 2018, 54, 1762-1765.

35 J. Chang, H. Li, T. Hou, W. Duan and F. Li, *Biosens. Bioelectron.*, 2018, 104, 152-157.

36 B. Liu, Z. Sun, P. J. Huang and J. Liu, *J. Am. Chem. Soc.*, 2015, 137, 1290-1295.

37 Z. Qi, L. Wang, Q. You and Y. Chen, *Biosens. Bioelectron.*, 2017, 96, 227-232.

38 H. C. Chang and J. A. Ho, *Anal. Chem.*, 2015, 87, 10362-10367.

39 J. Yuan, Y. Cen, X. J. Kong, S. Wu, C. L. Liu, R. Q. Yu and X. Chu, *ACS Appl. Mater. Interfaces*, 2015, 7, 10548-10555.

40 J. Chen, X. Ji and Z. He, *Anal. Chem.*, 2017, 89, 3988-3995.

41 H. Lu, C. Yu, S. Quan and S. Xu, *Analyst*, 2019, 144, 1153-1158.

42 Y. Zhang, E. T. Lee, R. B. Devereux, J. Yeh, L. G. Best, R. R. Fabsitz and B. V. Howard, *Hypertension*, 2006, 47, 410-414.

43 W. Zhang, X. Li, X. Xu, Y. He, F. Qiu, J. Pan and X. Niu, *J. Mater. Chem. B*, 2019, 7, 233-239.

44 J. Li, Y. Li, S. A. Shahzad, J. Chen, Y. Chen, Y. Wang, M. Yang and C. Yu, *Chem. Commun.*, 2015, 51, 6354-6356.

45 J. L. Ma, B. C. Yin, X. Wu and B. C. Ye, *Anal. Chem.*, 2017, 89, 1323-1328.

View Article Online
DOI: 10.1039/C9AN00395A

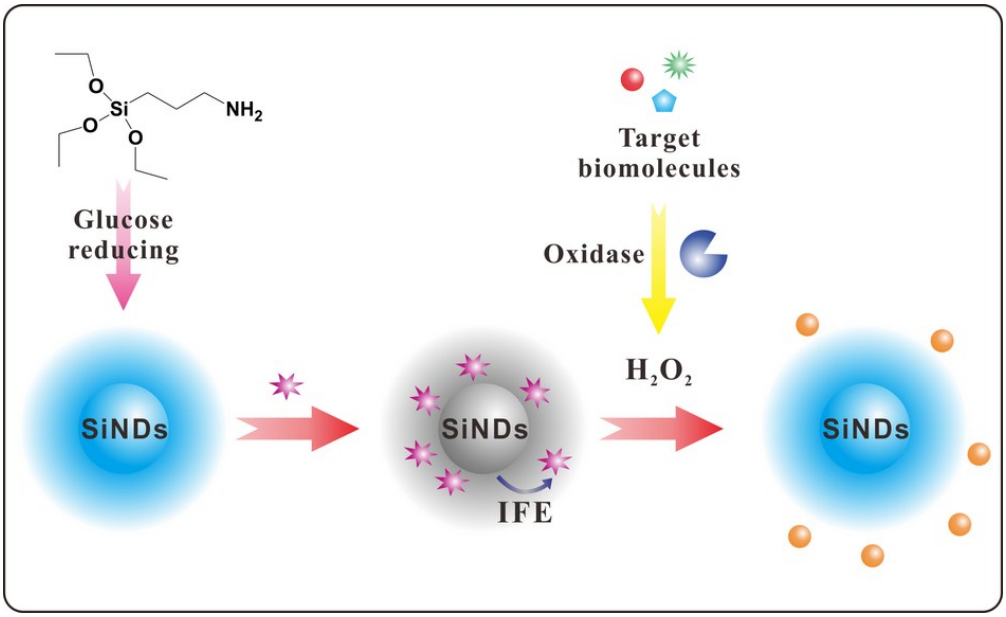

80x48mm (300 x 300 DPI)